Anomalous dynamics of water confined in MCM-41 at different hydrations

2010 J. Phys.: Condens. Matter 22 284102

(http://iopscience.iop.org/0953-8984/22/28/284102)

J. Phys.: Condens. Matter **22** (2010) 284102 (8pp) doi:10.1088/0953-8984/22/28/284102

Anomalous dynamics of water confined in MCM-41 at different hydrations

P Gallo[1], M Rovere[1] and S-H Chen[2]

[1] Dipartimento di Fisica, Università 'Roma Tre', Via della Vasca Navale 84, I-00146 Roma, Italy
[2] Department of Nuclear Science and Engineering, Massachusetts Institute of Technology, Cambridge, MA 02139, USA

E-mail: gallop@fis.uniroma3.it

Received 1 December 2009, in final form 8 March 2010
Published 21 June 2010
Online at stacks.iop.org/JPhysCM/22/284102

Abstract
We present the results of molecular dynamics simulations on water confined in a silica pore of 15 Å modelled to mimic the MCM-41 structure. We focus on the dynamical properties of water for different hydration levels of the pore. Density profiles show a well-defined double-layer structure close to the surface. From the analysis of the layers we find that water molecules close to the substrate show an anomalous diffusion which is connected to the behaviour of the residence time distribution. The interaction with the substrate induces temporal disorder. As a consequence strong deviations are found from the Markovian processes that usually determine the long-time diffusion properties. The residence time distribution of the water molecules in the inner part of the pore, far from the hydrophilic surface, is compatible with a Markovian process.

(Some figures in this article are in colour only in the electronic version)

1. Introduction

The study of water at interfaces and in confined geometries is certainly a topic of wide interest for the many connections with important phenomena in chemistry, biology and technological applications where water is in contact with different hydrophobic and/or hydrophilic substrates, see, for example, [1–15]. The interest in this kind of study is twofold. From one side the problem is to understand to what extent confined water can reproduce the properties of bulk water under supercooled conditions that are quite difficult to reach in experiments for the bulk [16, 17]. On the other side, it is of interest to characterize the properties of interfacial water which plays a crucial role in chemical and biological processes. In contact with proteins, for instance, water is important in fundamental processes like protein folding [18].

The possibility of performing experiments on supercooled confined water, where crystallization can more easily be avoided, has become a common idea of scientists interested in the anomalies of water. In fact, anomalous increases of thermodynamic response functions, like isothermal compressibility and isobaric specific heat, and of dynamic quantities are observed in water on approaching a singular but experimentally inaccessible temperature of about 227 K at ambient pressure. The deep supercooled region of water is not accessible with experiments because of homogeneous nucleation [16, 17, 19]. This nucleation could be possibly experimentally suppressed in water free of all impurities [20], but this is a quite difficult condition to obtain. Experiments have shown that supercooled conditions that are inaccessible in bulk water can be reached under confinement [21–23]. In the last few years a number of experiments have been performed on water confined in MCM-41, a material composed of silica nanopores with diameters of 14–20 Å [24–28], in order to investigate the connection between the glassy dynamics and the possible existence of a liquid–liquid phase transition in supercooled water [29–31].

In a series of computer simulations on water confined in Vycor [5, 6, 32, 33] it has been shown that in hydrophilic environments water forms hydrogen bonds (HB) with the atoms of the substrate with the consequent distortion of the HB network, but if water is confined in a large enough space at a high enough hydration level it is possible to recover properties similar to bulk water in the set of molecules which are far enough from the substrate to be almost unperturbed, the free water. The perturbation can extend for distances of the order of 4–6 Å from the substrate as also confirmed by recent results on water close to biological surfaces [34]. While free water shows a behaviour similar to the bulk, large changes are found

in the structure and dynamics of water close to the surfaces, the bound water [5, 6, 35, 36].

Sometimes in the interpretation of experiments and computer simulation on confined water the distinction between free and bound water is not taken into account, with the consequence of mixing up the effects of different types.

While the study of free water is connected to research on supercooled bulk water, bound water is of interest because it shows very peculiar properties, due to the strong interaction with the environment.

Interesting anomalous phenomena are frequently observed when water is close to disordered polar surfaces or near biomolecules, like: (i) a strong slowing down of the dynamics already at ambient temperature [5, 6] and (ii) a sublinear behaviour of the mean square displacement [3, 34–43].

In a recent series of molecular dynamics (MD) studies of SPC/E water confined in an MCM-41 pore with a diameter of 15 Å we found that also in such a narrow pore it is possible to distinguish between the two different behaviours of free and bound water. For the highest hydration investigated we showed that the dynamical behaviour upon supercooling of free water is consistent with the behaviour of bulk water [44]. In particular we found for free water upon supercooling a fragile to strong crossover in the relaxation time observed in QENS experiments on water in MCM-41 [24, 25, 27] and in simulations in bulk water [31].

In this paper we consider the bound water at a low hydration level where most of the water molecules reside in layers close to the substrate and we compare its behaviour with the high hydration case.

We also compare the properties obtained here for water in MCM-41 with the case of water at low hydration in Vycor, where the pore radius is larger, 20 Å [35, 36], and the water molecules have more available space to diffuse towards the region close to the centre of the pore.

In section 2 we describe the methodology of our computer simulation. In section 3 we discuss how water is structured inside the pore for different hydrations. In section 4 we briefly describe the dynamics results just published for the high hydration case and the connection between free and bulk water [44]. Then in section 5 we present the results for the diffusion and the residence time distribution of confined water for different hydrations performing a layer analysis. Section 6 is devoted to conclusions.

2. Computer simulation of confined water

In our computer simulation study we consider the problem of water confined in an MCM-41 structure. MCM-41 is a silica porous material and is one of the most commonly used mesoporous substrate for studying confined fluids, since it is very well characterized with pores periodically arranged in space [45]. Different MCM-41 samples are used in experiments, characterized by the different procedures involved in obtaining the final configuration of the material. In our simulations we study water molecules confined in a single pore modelled to catch the main features of the MCM-41 system.

Table 1. Bridging oxygens (bO), non-bridging oxygens (nO), silicons (Si) and acidic hydrogens (aH) potential parameters [32].

	q (e)	σ (Å)	ϵ (K)
bO	−0.629	2.70	230
nO	−0.533	3.00	230
Si	1.283	—	—
aH	0.206	—	—
Ow	−0.848	3.17	78.2
Hw	0.424	—	—

In order to perform MD simulations in a normal box with periodic boundary conditions we built, as a starting point, a silica cube, where a cylindrical pore of appropriate size can be carved. The silica system is simulated with the Vessal *et al* potential [46]. We start the MD simulation from a β-cristobalite crystal of silica. The cube of silica has length $L = 42.78$ Å. The MD is performed at constant volume. The crystal is melted and the liquid SiO_2 is equilibrated at 1000 K. The system is quenched to 300 K to obtain a glassy phase of silica. Inside the silica glass cube a cylindrical pore of 15 Å diameter was carved. Then the system was relaxed with an additional MD run. In the final configuration at the surface of the pore there are bridging oxygens (bO) with two silicon neighbours and non-bridging oxygens (nO) with only one silicon neighbour. The nO were saturated with acidic hydrogens (aH). The axis of the cylindrical pore is assumed along the z direction. Periodic boundary conditions are applied along the three directions of the silica cube.

The water molecules are inserted in the centre of the pore in a starting lattice configuration. The water is modelled with the SPC/E three-site potential, where one site (Ow) represents the oxygen and the other two (Hw) the hydrogens. The interaction of the water sites (Ow, Hw) with the atoms of the substrate (Si, bO, nO, aH) is determined by an effective potential already used in previous simulations [32]. The SPC/E and the water–substrate potentials are given by a combination of Lennard-Jones and Coulombic potentials defined as

$$U_{ij}(r) = \frac{q_i q_j}{r} + 4\epsilon_{ij}\left[\left(\frac{\sigma_{ij}}{r}\right)^{12} - \left(\frac{\sigma_{ij}}{r}\right)^{6}\right]. \quad (1)$$

The force field is defined by the parameters reported in table 1. We used the Lorentz–Berthelot mixing rules for the Lennard-Jones part of the interaction:

$$\sigma_{ij} = \tfrac{1}{2}(\sigma_i + \sigma_j) \quad (2)$$

$$\epsilon_{ij} = \sqrt{\epsilon_i \epsilon_j}. \quad (3)$$

The shifted force method was adopted with a cutoff at 9 Å for all the interactions since long runs of simulation are needed for the study of dynamical properties in regions where systems approach the glass transition. The choice of the size of the initial box length as $L = 42.78$ Å was done by taking into account the cutoff of the potentials and the minimum image convention.

The temperature is taken under control during equilibration by means of the Berendsen thermostat. Production runs are done in the microcanonical ensemble.

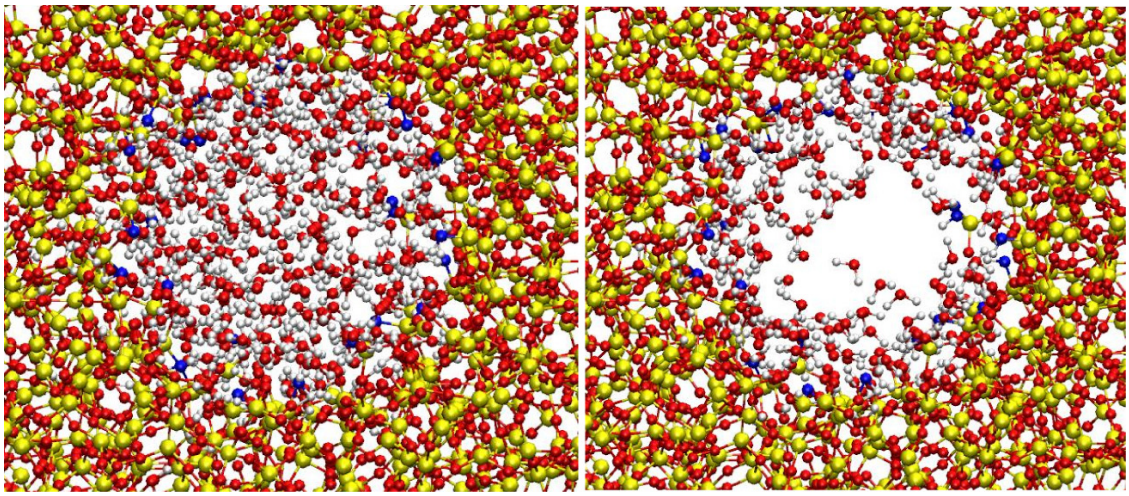

Figure 1. Projections in the xy plane of the snapshots of the water configuration inside the silica cavity at $T = 300$ K. A portion of the silica surface is shown. The larger spheres are silicon atoms. Left: $N_w = 380$, right: $N_w = 216$.

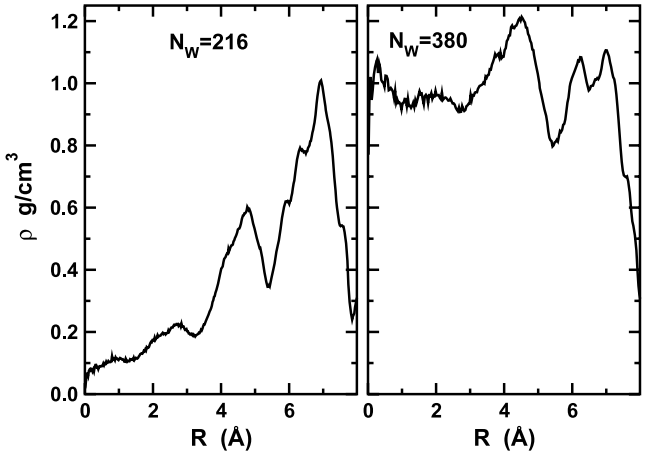

Figure 2. Density profiles of water oxygens along the MCM-41 pore. In the panel on the left: low hydration case, $N_w = 216$. In the panel on the right: high hydration case, $N_w = 380$. The density profiles are drawn up to where the substrate atoms start to be present.

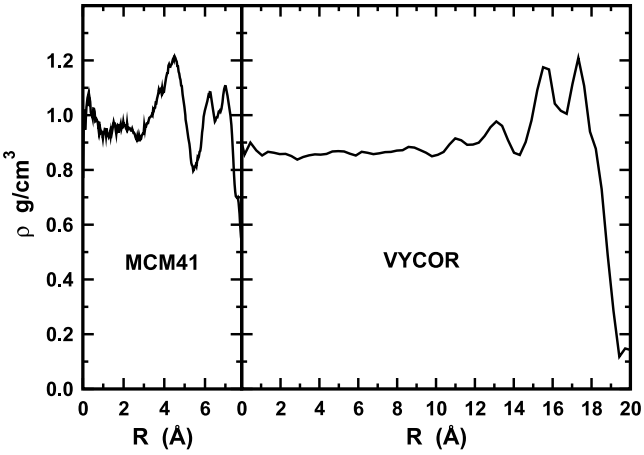

Figure 3. Density profiles of water oxygens along the pore. In the panel on the left: water in MCM-41 with $N_w = 380$. In the panel on the right: water confined in Vycor with $N_w = 2600$ hydration. Proportion between the pores have been respected in the x axis. The density profiles are drawn up to where the substrate atoms start to be present.

In this paper we report results obtained with a number of water molecules $N_w = 216$, low hydration case, and $N_w = 380$, high hydration case.

3. Structure

The snapshots of our systems reported in figure 1 show that in the low hydration case the water molecules are mainly attached at the surface.

The density profiles of water oxygens in MCM-41 along the radius of the pore, $R = \sqrt{x^2 + y^2}$ in our geometry, for the two different hydrations are reported in figure 2.

We observe that in both cases a double-layer structure close to the surface is formed. For $N_w = 380$ the water molecules are distributed more homogeneously in the region close to the centre of the pore.

We also compare in figures 3 and 4 the density profiles of oxygens of water confined in MCM-41 with the density profiles of oxygens of water confined in Vycor. The latter profiles were obtained in previous simulations [5, 6, 35, 36], where the pore of Vycor was modelled with a diameter of 20 Å.

In figure 3 we show the two high hydration cases and we note that the formation of a double-layer structure close to the substrate is more evident in MCM-41 and that approaching the centre of the pore large differences are visible. The density profile in Vycor is more homogeneous with respect to MCM-41.

In more detail the first layer of water in MCM-41 is shifted closer to the substrate. The second layer is also shifted towards the surface in MCM-41 and it is more well defined than in Vycor. These findings show differences in the composition of the surfaces offered to water in the two cases. Similar considerations can be applied to figure 4 where we show the two low hydration cases. In particular, the double-layer

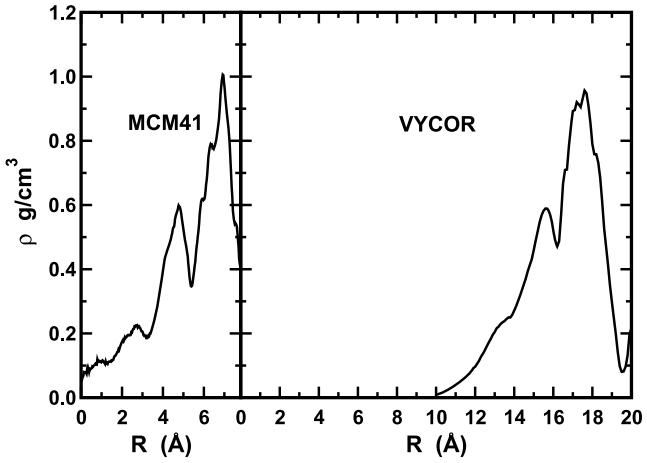

Figure 4. Density profiles of water oxygens along the pore. In the panel on the left: water in MCM-41 with $N_w = 216$. In the panel on the right: water confined in Vycor with $N_w = 1000$ (in the layer $0\ \text{Å} < r < 10\ \text{Å}$ there are, on average, no molecules). Proportion between the pores have been respected in the x axis. The density profiles are drawn up to where the substrate atoms start to be present.

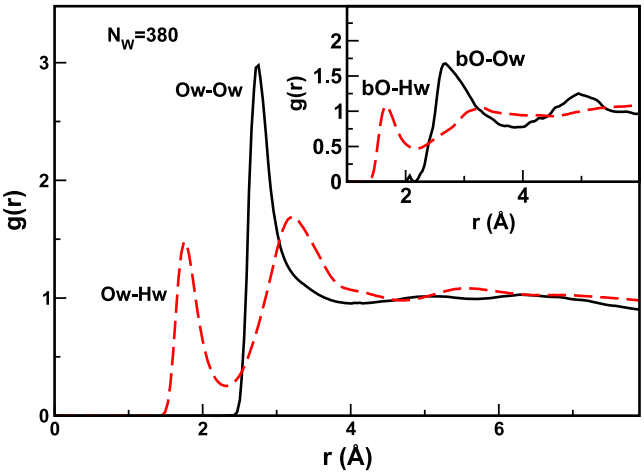

Figure 5. Radial distribution function for $N_w = 380$ at $T = 300$ K. The water–water OO and OH contributions are drawn in the main frame. In the inset we show the RDF between bridging oxygens and water.

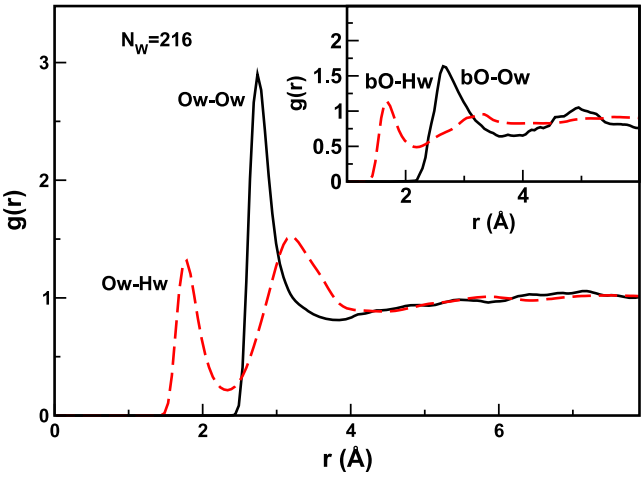

Figure 6. Radial distribution function for $N_w = 216$ at $T = 300$ K. The water–water OO and OH contributions are drawn in the main frame. In the inset we show the RDF between bridging oxygens and water.

structure is still visible in both systems and the difference in the peak positions remains the same as in the high hydration cases.

We remark that there is a strong difference between the two pores due to the large amount of available space for the diffusion of molecules in Vycor: to be precise, the Vycor pore has a region, $0\ \text{Å} < R < 12\ \text{Å}$ in the figure, that offers space that is not available in the more restricted pore of MCM-41.

With the same procedure used for water in Vycor [33] we calculated the radial distribution functions (RDF) of water in MCM-41. In figures 5 and 6 we show the RDF g_{OwOw}, g_{OwHw} and g_{bOOw}, g_{bOHw} calculated at $T = 300$ K for the low and high hydration cases. The g_{OwOw} and g_{OwHw} show in both cases that the hydrogen bond network is present. At high hydration we note that the second shell of oxygens in the g_{OwOw} is less defined with respect to bulk water but still visible. At lower hydration this second shell is not longer visible, indicating that the hydrogen bond network is distorted since all the water molecules are close to the surface. In the inset the RDF of the water oxygens with the bridging oxygens of MCM-41 show the formation of hydrogen bonds between the water molecules and the surface atoms. From the comparison of the g_{bOOw}, g_{bOHw} at the two hydrations we observe that this effect is independent from the hydration of the pore.

4. Layer analysis and dynamical behaviour of confined water

In a recent study [44] performed on the dynamics of the high hydrated pore, $N_w = 380$, we have shown that, similar to water in Vycor [5, 6], the dynamics of water inside the MCM-41 pore is like that of bulk water provided that we perform a layer analysis of the density correlator. This result is remarkable since the pore of MCM-41 is much smaller with respect to that of Vycor.

The dynamical behaviour of fluids can be described in terms of the self-density correlation function (SISF), which is the Fourier transform of the distribution function of the single-particle positions in space. This quantity contains all the information on the single-particle dynamics. In liquids under normal conditions the SISF is expected to decay at long time as an exponential function (Debye regime). In liquids upon supercooling the so-called caging phenomenon starts to appear. After the short-time ballistic regime the particle remains for a certain time trapped inside the cage of the nearest neighbour. This can be detected in the SISF from the appearance of a plateau. After the time represented by the length of the plateau the particle can escape from the cage and the Brownian regime is recovered [47]. The slow decay of the SISF can be fitted with a stretched exponential function:

$$f_Q e^{-(t/\tau)^\beta}. \tag{4}$$

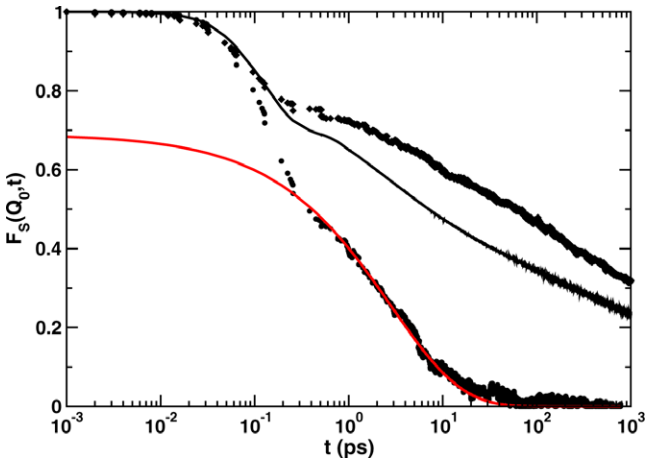

Figure 7. Self-intermediate scattering functions of the oxygen atoms of water at $T = 300$ K for $N_w = 380$. Continuous line: total SISF, filled circles: SISF for the inner shells, filled diamonds: SISF for the outer shells, light line: fit to the stretched exponential function, see equation (4), where $f_Q = 0.69$, $\tau = 2.84$ and $\beta = 0.58$.

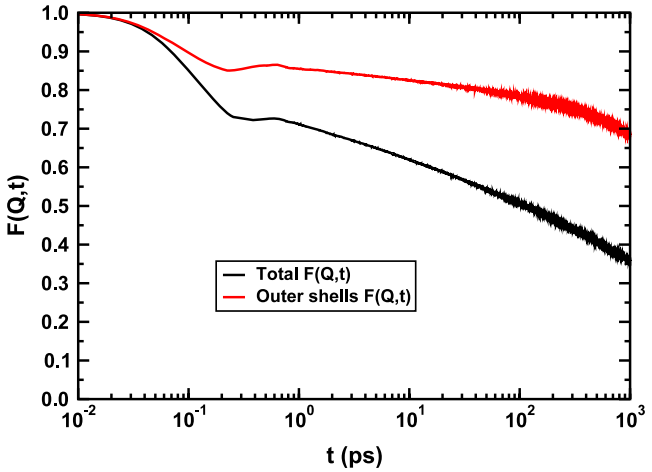

Figure 8. Total and partial self-intermediate scattering functions of the oxygen atoms of water at $T = 300$ K for $N_w = 216$. The total function are calculated for all the molecules, while the partial functions are calculated for the outer shells (see text). The SISF are calculated at Q_0, the maximum of the site–site structure factor of the oxygens.

In figure 7 we report the SISF of water in MCM-41 calculated at $T = 300$ K for the high hydration case. The three curves shown represent the total contribution to the correlator, the contribution coming from the inner shells, which are defined in the region 0 Å $< R <$ 5.5 Å [44], and the contribution coming from the outer shells $R >$ 5.5 Å.

The SISF are calculated at Q_0, the maximum of the site–site structure factor of the oxygens where the caging phenomenon is best evident on the correlator.

The total SISF could not be fitted with a stretched exponential function because it contains both the contribution of water close to the hydrophilic substrate and of water not in contact with the surface. The inner shell contribution can be fitted with the stretched exponential instead and the fit is also reported in the figure.

In our previous study on the high hydration we have shown that, upon supercooling, water contained in the inner layers, free water, behaves as bulk water, showing for the first time that the results of the numerous neutron scattering experiments on water in MCM-41 samples are valid to assess the bulk behaviour [44]. In particular, upon supercooling water undergoes a fragile to strong transition typical of glass formers at a temperature which in water coincides with the crossing of the Widom line. The latter is an important thermodynamics locus that signals the presence of a critical point, the liquid–liquid critical point in the case of supercooled water [31, 48].

In the following we focus on the dynamics of water close to the surface of the pore. The outer shell correlators cannot be fitted with the stretched exponential function neither for the high hydration case, shown in figure 7, nor for the low hydration case. In figure 8 we report the total and the outer shell $F_S(Q, t)$ for the low hydration case. The two-step relaxation scenario is still evident but we note that in this case all the water molecules are extremely slow. This is due to the fact that all of them reside in layers close to the substrate and the system is a prototype for studying bound water. In the next section we analyse on the diffusion properties and the residence time of bound water.

5. Anomalous diffusion and residence time distribution

In liquids at normal conditions the mean square displacement (MSD) $\langle r^2 \rangle = \langle x^2 \rangle + \langle y^2 \rangle + \langle z^2 \rangle$ shows a rather general behaviour where $\langle r^2 \rangle \sim t^2$ for short times, the ballistic regime, and $\langle r^2 \rangle \sim t$ in the long time limit, the Brownian regime. According to Einstein's relation in the Brownian limit

$$\langle r^2 \rangle = 6Dt \tag{5}$$

where D is the diffusion constant of the system.

In liquids upon supercooling the caging phenomenon, described in the previous section, affects the MSD behaviour at intermediate times. In the plot of $\langle r^2 \rangle$ versus t this effect is shown by the presence of a plateau. After the time represented by the length of the plateau the particle can escape from the cage and in the long time limit restores the Brownian regime [47].

Generally speaking, the Brownian regime is connected to Markovian processes where the diffusion of a particle takes place as a succession of independent moves; at each temporal step the particle loses memory of the previous dynamics. The distribution of the time intervals between the successive displacements in the Markovian processes is very narrow and the distribution function of the single-particle positions in space is a Gaussian and the calculation of its second moment gives Einstein's relation [49]. Correspondingly the residence time distribution (RTD) of the diffusing particle decays at long time as an exponential [50, 37, 38].

In the literature, violations of this behaviour in the long time limit have been reported. The MSD does not grow linearly with time as in the Brownian motion and shows an asymptotic

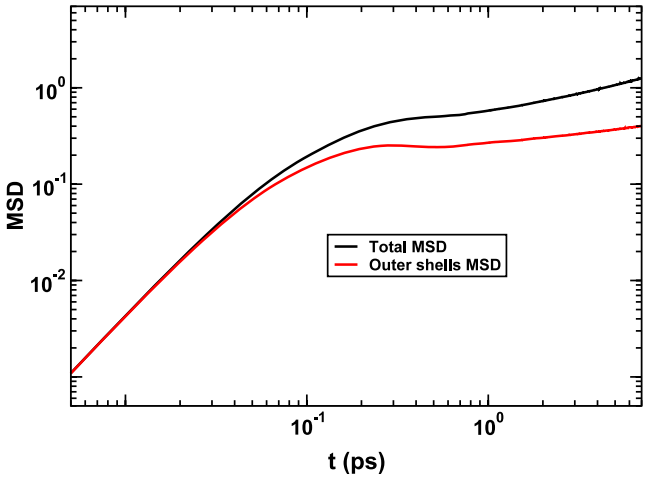

Figure 9. Total and partial MSD of the oxygen atoms of water at $T = 300$ K for $N_w = 216$. The total MSD is calculated for all the molecules, while the partial MSD is calculated for the outer shells.

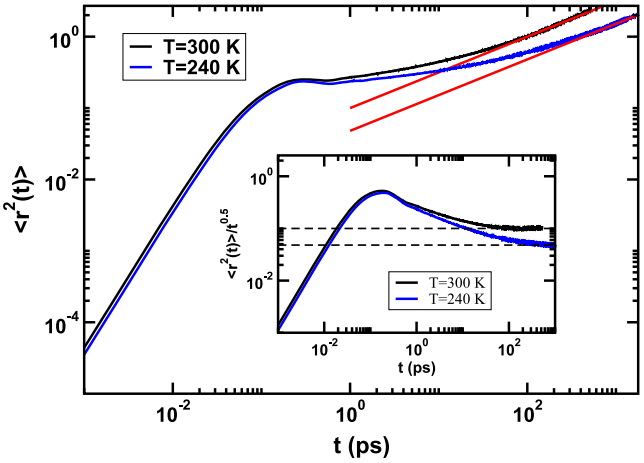

Figure 10. MSD of the outer shells for the low hydration $N_w = 216$ at temperatures $T = 300$ and 240 K. Straight lines are fits to the subdiffusion behaviour. Both lines have a slope of 0.5. In the inset the MSD are normalized to $t^{0.5}$ to see the convergence to the sublinear behaviour.

sublinear behaviour [3, 35–39, 34, 40–43]. This phenomenon is particularly interesting in the case of a complex substrate, as biomolecules have [37, 38],

The anomalous diffusive behaviour of the MSD in the long time limit

$$\langle r^2 \rangle \sim t^{\alpha} \tag{6}$$

with $\alpha \neq 1$ can be related to the analytic form of the RTD $\psi(t)$ [50, 51] that shows a power law decay at long times as a consequence of the broadening of the distribution of the time intervals [50]. Phenomenologically this broadening can be connected to the presence of a disordered substrate which prevents the diffusion of a particle from being generated by a succession of independent moves at long time.

In figure 9 the MSD at $T = 300$ K for the oxygen atoms of water in the low hydration case is shown. The quantities are calculated for all the molecules in the simulation cell and for the molecules in the outer layer (or outer shell).

From the figure it is evident that already at ambient temperature the MSD shows the onset of a cage effect, observed around 0.1 ps. The plateau, due to the rattling effect of the molecule inside the nearest-neighbour cage, is clearly visible.

Nonetheless, unlike most liquids undergoing a glass transition, bulk water included, the MSD of the interfacial water in MCM-41 after the plateau does not enter in the Brownian regime. At least on the timescale for which the system is observed the total and the outer shells MSD show a sublinear behaviour with $\alpha < 1$. By fitting the asymptotic branch of the MSD we found for $T = 300$ K $\alpha = 0.75$ for the total MSD and $\alpha = 0.5$ for the outer shell MSD. Now we concentrate our analysis on interfacial water.

In figure 10 the MSD of the outer layers at the ambient temperature and at $T = 240$ K are reported together with the fitting power law at long time. The onset of the cage effect appears at practically the same time, at lower temperature the particle is trapped in the cage for a slightly longer time than at ambient temperature. For both temperatures an exponent $\alpha \approx 0.5$ is found, therefore the exponent α does not appear to depend on the temperature. Similar results were found for water in Vycor [36].

As mentioned above, phenomena of anomalous diffusion, and in particular subdiffusion, are characteristic of interfacial water and they can be interpreted in terms of temporal disorder with a modulation of the times between the successive moves of the particle, in our case the centre of mass of the water molecule, represented by the oxygen atoms. In order to further verify this interpretation we analyse in the following the residence time distribution.

A power law behaviour of the RTD is therefore to be related to anomalous diffusion. The residence time of water in a layer is obtained for our case by calculating for each molecule i which is found in the layer λ at the initial time the interval of time $\tau_{i\lambda}$ for which the molecule stays in the shell. The distribution function of the residence time is then obtained by averaging over the $\tau_{i\lambda}$ of all the molecules in the layer λ.

The residence time distribution $\psi(t)$ for the outer shell for the hydration $N_w = 216$ is reported in figure 11 for the same temperatures for which the MSD is shown, $T = 300$ and 240 K.

It is evident the power law decay of the tail at long time is

$$\psi(t) \sim t^{-\mu}. \tag{7}$$

The exponent found is $\mu \approx 1.5$. This exponent can be compared with the results obtained for water in Vycor for the hydration $N_w = 1000$ and $N_w = 1500$. The RTD in the layer 14 Å $< R <$ 20 Å shows in both cases a power law with $\mu \sim 1.5$ at $T = 300$ and 240 K.

For the same hydrations in Vycor the RTD of the water molecules in the layer 0 Å $< R <$ 14 Å results in having an exponential decay.

If the residence time distribution is related to the subdiffusive behaviour of MSD, the exponent α in (6) is connected to μ by the relation [36–38, 50]

$$\alpha = \mu - 1. \tag{8}$$

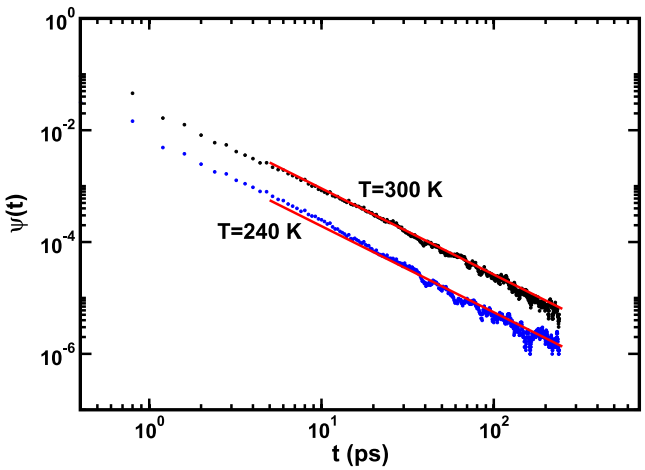

Figure 11. Log–log plot of the residence time distribution as a function of time for the oxygen atoms of water. The curve for $T = 240$ K is shifted by a constant factor for clarity. The bold lines are fits with the power law formula $\psi(t) = at^{-\mu}$ with $\mu = 1.5$.

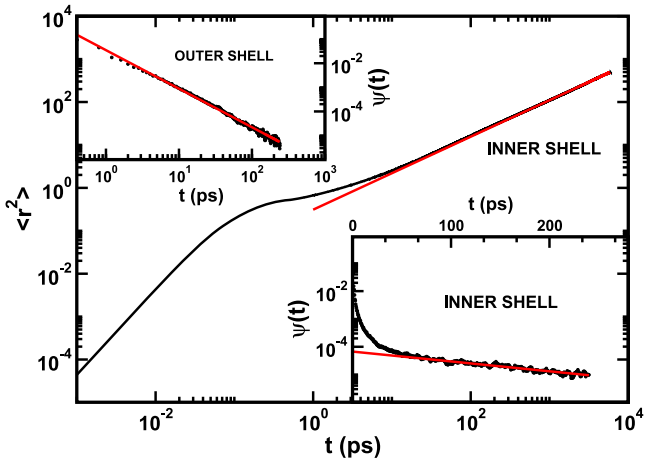

Figure 12. Log–log plot of the MSD for the inner shells of the system with $N_w = 380$ at $T = 300$ K. In the inset at the bottom: linear–log plot of the RTD for the inner shells fitted with an exponential decay. In the inset at the top: log–log plot of the RTD for the outer shells fitted with a power law decay.

In the case of $N_w = 216$ the values obtained of $\alpha = 0.5$ from our MSD are consistent with (8). This check is important because from the regularity of the slope in figure 11 we are confident that also the MSD has reached an asymptotic behaviour.

In the MCM-41 pore we studied also the dynamics of the inner shells for the high hydration case of $N_w = 380$ [44]. In figure 12 we report in the main frame the MSD for the inner shells, The MSD shows, as in the low hydration case, a cage effect. Now the difference is that, in the long-time limit, the behaviour is more similar to the Brownian regime. The exponent is still sublinear, $\alpha \approx 0.85$, but much closer to $\alpha = 1$ of the Brownian regime.

Looking at the RTD we observe that, as reported in the inset at the bottom in figure 12, the long-time decay is exponential, as expected in the Brownian case and in agreement with the inner shells analysis of the Vycor case [36]. The RTD analysed for the outer shells decays instead with a power law, confirming the general behaviour in the case of the diffusion of particles close to disordered substrates.

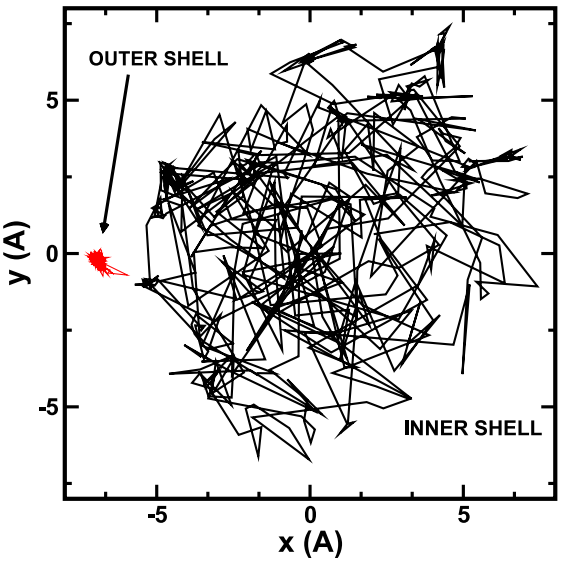

Figure 13. Trajectories of two molecules in the water at high hydration belonging to the free and the bound water reported in the plane x–y of the simulation cell.

From this point of view, to get an idea of the differences in the diffusion between the free and the bound water in figure 13 partial trajectories of two molecules are reported for the system with $N_w = 380$. The particle in the free water spread out in all the simulation cell while in the bound water it is possible to find molecules, like the one tracked in the figure, which are trapped very close to the surface, at least for the time it has been observed.

The substantial differences in the RTD behaviours can be ascribed to the different dynamics of the molecules. It is clear that the *free* molecule is able to perform a random walk in the long-time regime, while for the *bound* molecule we can hypothesize a non-Markovian process of diffusion due to the restricted region in the phase space.

6. Conclusions

The subdiffusive behaviour is found in different situations where water is confined or in contact with different substrates. The problem was first discussed in connection with diffusion of electrons and holes in amorphous inorganic and organic materials [50]. More recently the phenomenon has become of relevant interest in the study of the dynamics of water at interfaces with biological macromolecules [37, 40].

We reported and discussed here results of computer simulations performed on water confined in a nanopore of MCM-41. We observed a slowing down of the dynamics with a similarity between the confined water and a supercooled liquid already at ambient temperature. For the high hydration case it is possible to separately analyse bound and free water. Free water behaves like bulk water as far as cooperative properties are concerned [44]. We focused here in particular on the phenomenon of the anomalous diffusion. For the hydration levels and the time intervals explored in our MD simulation the molecules which are in the shells close to the substrate

do not enter in the Brownian regime when the cage relaxes. This is also reflected in the power law decay at long time of the residence time distribution for the high hydration, where it is possible to perform an analysis of the inner shells: the Brownian regime is almost recovered for the MSD while the RTD decays according to the Markovian approximation.

In spite of the much smaller diameter of the MCM-41 pore with respect to Vycor, results found in the two systems are similar. This shows that, for water close to a hydrophilic surface, the existence of an interfacial shell with a subdiffusive behaviour presents general features. It is possible to infer that, in spite of the differences in the size and the arrangement of the pore surface, a kind of general behaviour is found for bound water by considering not only the case of water in Vycor and MCM-41, but also that similar behaviours are found for water at contact with biomolecules [37, 38], in particular the same exponent for the RTD decay, $\mu \sim 1.5$, is found.

Therefore it is of interest to perform further experiments and theoretical studies aimed at singling out the general features of the interfacial water phenomena.

Acknowledgments

This paper is a contribution that concerns recent progresses in the field of computer simulations of water discussed at the CECAM workshop 'Modeling and Simulation of Water at Interfaces from Ambient to Supercooled Conditions' supported by ESF-Simbioma and CECAM.

The research at MIT is supported by DOE grants DE-FG02-90ER45429. PG and MR gratefully acknowledge the computational support of the Roma Tre INFN-GRID.

References

[1] Debenedetti P G 1977 *Metastable Liquids: Concepts and Principles* (Princeton, NJ: Princeton University Press)
[2] Lombardo G, Giovambattista N and Debenedetti P G 2009 *Faraday Discuss.* **141** 359
[3] Romero-Vargas Castrillón S, Giovambattista N, Aksay I A and Debenedetti P G 2009 *J. Phys. Chem.* B **113** 7973 and references therein
[4] Giovambattista N, Rossky P J and Debenedetti P G 2009 *J. Phys. Chem.* B **113** 13723
[5] Gallo P, Rovere M and Spohr E 2000 *Phys. Rev. Lett.* **85** 4317
[6] Gallo P, Rovere M and Spohr E 2000 *J. Chem. Phys.* **113** 11324
[7] Gallo P 2000 *Phys. Chem. Chem. Phys.* **2** 1607
[8] Rovere M and Gallo P 2003 *Europhys. J.* E **12** 77 and references therein
[9] Zhang Q Y, Chan K Y and Quirke N 2009 *Mol. Simul.* **35** 1215
[10] Han S, Kumar P and Stanley H E 2008 *Phys. Rev.* E **77** 030201(R)
[11] Kumar P, Starr F W, Buldyrev S V and Stanley H E 2007 *Phys. Rev.* E **75** 011202
[12] Majolino D, Corsaro C, Crupi V, Venuti V and Wanderlingh U 2008 *J. Phys. Chem.* B **112** 3927
[13] Crupi V, Longo F, Majolino D and Venuti V 2006 *J. Phys.: Condens. Matter* **18** 3563
[14] Crupi V, Majolino D, Migliardo P, Venuti V and Mizota T 2004 *Mol. Phys.* **102** 1943
[15] Gordillo M C and Marti J 2007 *Phys. Rev.* B **75** 085406
[16] Stanley H E 1999 *Mater. Res. Bull.* **24** 22
[17] Debenedetti P G 2003 *J. Phys.: Condens. Matter* **15** R1670
[18] Ball P 2008 *Chem. Rev.* **108** 74
[19] Debenedetti P G and Stanley H E 2003 *Phys. Today* **56** (6) 40
[20] Speedy R J, Debenedetti P G, Smith S R, Huang C and Kay B D 1996 *J. Chem. Phys.* **105** 240
[21] Zanotti J-M, Bellisent-Funel M-C and Chen S-H 1999 *Phys. Rev.* E **59** 3084
[22] Bruni F, Ricci M A and Soper A K 1998 *J. Chem. Phys.* **109** 1478
[23] Ricci M A, Bruni F and Giuliani A 2009 *Faraday Discuss.* **141** 347
[24] Faraone A, Liu L, Mou C-Y, Yen C-W and Chen S-H 2004 *J. Chem. Phys.* **121** 10843
[25] Liu L, Chen S-H, Faraone A, Yen C-W and Mou C-Y 2005 *Phys. Rev. Lett.* **95** 117802
[26] Mallamace F, Broccio M, Corsaro C, Faraone A, Wanderlingh U, Liu L, Mou C-Y and Chen S-H 2006 *J. Chem. Phys.* **124** 161102
[27] Faraone A, Liu K-H, Mou C-Y, Zhang Y and Chen S-H 2009 *J. Chem. Phys.* **130** 134512
[28] Liu L, Faraone A, Mou C-Y, Yen C-W and Chen S-H 2004 *J. Phys.: Condens. Matter* **16** S5403
[29] Poole P H, Sciortino F, Essmann U and Stanley H E 1992 *Nature* **360** 324
[30] Poole P H, Sciortino F, Essmann U and Stanley H E 1993 *Phys. Rev.* E **48** 3799
[31] Xu L, Kumar P, Buldyrev S V, Chen S-H, Poole P H, Sciortino F and Stanley H E 2005 *Proc. Natl Acad. Sci. USA* **102** 16558
[32] Spohr E, Hartnig C, Gallo P and Rovere M 1999 *J. Mol. Liq.* **80** 165
[33] Gallo P, Ricci M A and Rovere M 2002 *J. Chem. Phys.* **113** 342
[34] Tobias D J, Sengupta N and Tarek M 2009 *Faraday Discuss.* **141** 99
[35] Gallo P, Rapinesi M and Rovere M 2002 *J. Chem. Phys.* **117** 369
[36] Gallo P and Rovere M 2003 *J. Phys.: Condens. Matter* **15** 7625
[37] Rocchi C, Bizzarri A R and Cannistraro S 1998 *Phys. Rev.* E **57** 3315
[38] Paciaroni A, Bizzarri A R and Cannistraro S 2000 *Phys. Rev.* E **62** 3991
[39] Sega M, Vallauri R and Melchionna S 2005 *Phys. Rev.* E **72** 041201
[40] Pizzitutti F, Marchi M, Sterpone F and Rossky P J 2007 *J. Phys. Chem.* B **111** 7584
[41] van Hijkoop V J, Dammers A J, Malek K and Coppens M-O 2007 *J. Chem. Phys.* **127** 087101
[42] Garberoglio G, Sega M and Vallauri R 2007 *J. Chem. Phys.* **126** 125103
[43] Chowdhary J and Ladanyi B M 2008 *J. Phys. Chem.* B **112** 6259
[44] Gallo P, Rovere M and Chen S-H 2010 *J. Phys. Chem. Lett.* **1** 729
[45] Muroyama N, Yoshimura A, Kubota Y, Miyasaka K, Ohsuna T, Ryoo R, Ravikovitch P I, Takata M, Neimark A V and Terasaki O 2008 *J. Phys. Chem.* C **112** 10803
[46] Vessal B, Amini M and Catlow C R A 1993 *J. Non-Cryst. Solids* **159** 184
[47] Götze W 2009 *Complex Dynamics of Glass-Forming Liquids: a Mode-Coupling Theory* (Oxford: Oxford University Press)
[48] Franzese G and Stanley H E 2007 *J. Phys.: Condens. Matter* **19** 205126
[49] Hansen J P and Mc Donald I R 2006 *Theory of Simple Liquids* 3rd edn (New York: Academic)
[50] Scher H and Montroll W 1975 *Phys. Rev.* B **12** 2455
[51] Bettin R, Mannella R, West B J and Grigolini P 1995 *Phys. Rev.* E **51** 212